Research Progress and Application of Thin-walled Box-shaped Tube Folding Theory under Axial Crushing

Jingdong Liu, Benying Wu*, Xiwu Zhou, Weifeng Rong

Foshan University, 528000, Foshan, China

Abstract: Thin-walled box-shaped tubes, which feature good energy absorption and have a wide range of applications, can be flexibly combined with various buffer materials to form a combined energy consumption structure; However, in view of the complexity of the buffer forms when subjected to axial compression, there is still much room for intensive study in the calculation of the folding method, energy consumption and average force of the tube body during axial crushing. Based on the folding mode and spatial buckling behavior theory of box-shaped tube under axial compression, it not only sorts out the literature on the establishment and improvement process of super-folding theory, but also makes a comparison and analysis of the advantages and disadvantages of the classical method in the calculation of critical buckling force of box-shaped tubes. Moreover, it gives an overview on the common application methods of tube engineering and theoretical progress in terms of the application of box-shaped tubes, as well as makes a summary of the prospect and improvement of box section tube application in civil engineering at the end in this paper.

1 Introduction

Thin-walled box section tubes, which have suitable cushioning strength and high specific energy absorption because of its stability of energy consumption during axial crushing, are often made into various buffer devices to play the role of energy consumption and material enclosure. Not only can it independently form an efficient energy dissipation absorber, but also can combine with other energy consumption structures to form multilevel and multiform energy consumption systems[1-4]. Box-shaped tubes show different crushing patterns due to the constraints of adjacent sheets, as well as the width-thickness ratio and aspect ratio during axial crushing. The methods of solution of folding energy consumption model plays a crucial role in better applying thin-walled box-shaped tubes to practical engineering. Therefore, there is still a large research space in folding model and energy consumption calculation on account of the complexity of folding modes. Box section tubes have a variety of forms, and its combination of filling and lattice in space can better exert its performance. At present, many researchers have done detailed and comprehensive research on the space optimization of box tubes, and have also made corresponding improvements and extensions in the calculation modes.

Great importance is attached to the two aspects of energy consumption capability and crashworthiness in the design of the box-shaped tubes. In order to reach the goal of design and theoretical calculation, researchers tend to combine theoretical derivation, numerical simulation, experimental verification, finite element simulation and other methods. On the load displacement curve after the compression of the tube body, the curve can be divided into three stages according to the force characteristics, representing the three stages of the tube body crushing process, namely: the initial buckling stage, the platform stage, and the dense stage [5, 6], as can be seen in Fig. 1. At the same time, the researchers used various indicators related to energy consumption and crashworthiness so as to carry out a detailed comparison and analysis in an accurate way. As shown in Table 1, the comprehensiveness of the indicators and the definition of each energy dissipation is a prerequisite for accurate analysis of the crashworthiness and optimization of the tube body.

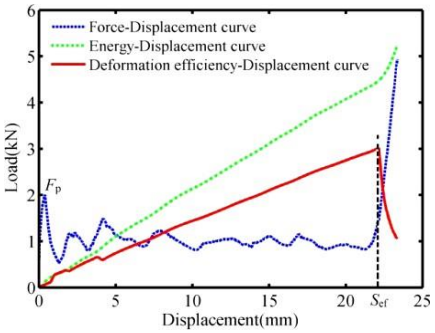

Fig. 1 Three stage diagram of axial compression curve of pipe fittings and related parameters [6]

In the field of civil engineering, thin-walled metal structures are of essential significance in shock buffering in key positions of bridges and house buildings. For

* Corresponding author: wubenying163@163.com

example, the metal tube box can play an effective protective role when ship-bridge collision, vehicle-column impact and other accidents occur[9]. However, the manifestation of axial crushing of thin-walled metal tubes is relatively complex, and the shape of the tube cross-section, the aspect ratio of the tube body, as well as the lattice form of the tube will also exert an influence on the folding mode and crashworthiness of the thin-walled tubes[10-12]. As a result, researchers have conducted numerous research on the crushing shapes and energy consumption of thin-walled tubes.

In this paper, it completes the work of sorting the calculation formula of the folding mode and energy consumption of thin-walled tubes proposed by previous researchers, and makes an analysis and screening of the critical force calculation method suitable for axial compression of box section tube in the calculation specification of the limit state of steel section. Meanwhile, in this paper, the calculation methods of box section tubes are classified and summarized, and the application prospects and challenges of box section tubes in civil engineering industry are analyzed after comparing the differences between box section tube application in vehicle protection measures and civil engineering protection.

Table 1. Related indicators on energy consumption and crashworthiness of box-shaped tube specimens[7, 8]

Indicator Name	Symbols or Abbreviations	Calculation Formula or Interrelationship	Annotation
Peak value of the initial Collapsing Force	P_I	/	The peak value of the initial crushing force is calculated by theoretical calculations or experimental curves.
Energy absorption	EA	$EA=\int_0^{\delta} F(x)dx$	obtained by load displacement curve integration
Average crushing force	P_m	$P_m=\frac{E_a}{\delta_a}$	δ_a refers to the compression stroke of the specimen before densification; E_a means the crushing energy consumption of the specimen before densification.
The efficiency of crushing force	CEF	$CEF=\frac{P_m}{P_I}\times 100\%$	the ratio between the peak value of initial crushing force and the average crushing force;
Effective stroke	ESR	$ESR=\frac{\delta_E}{L}$	δ_E is the effective compression stroke; L is the original length of the specimen.
Specific energy absorption	SEA	$SEA=\frac{EA}{m}$	unit mass of energy absorption

2 Theory of Axial Folding of Thin-Walled Box-Shaped Tube

2.1 Super-folding Element Theoretical Model

The spatial structure of box-shaped and thin-walled metal tube when folded axially is quite complex, so the researchers have put forward the box-shaped tube folding theory and improved it from different aspects by carefully observing its crushing space structure. Abramowicz et al.[13] were the first to propose the super-folding element theoretical model which includes two super-folding element types (Type I and Type II) through simulating the folding shapes of box-shaped tubes by origami and summarizing a large number of crushing experimental results. The super-folding element consists of 4 trapezoidal faces and 1 annular shell element, each of which represents a 1/4 segment of the tube body section at the height of the element as shown in Figure 2. For ease of description, the element height is set to 2H; The thickness of the tube wall is set to h; The angle between adjacent tube surfaces observed along the tube axis is set to $2\psi_0$; The width of both sides of the element is set to c1 and c2 respectively; The folding angle is set to α; The angle between the rotating tube surface and the tube angle line is set to β; The deflection angle of the tube angle is set to γ, and more parameters and their correlations are shown in Table 2.

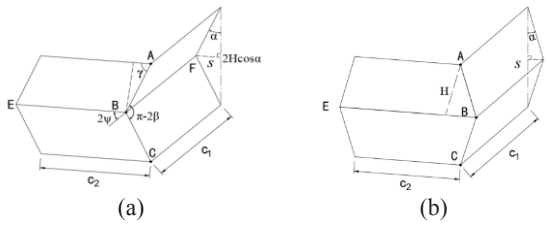

Fig. 2 Types of folding element ;(a) Type I; (b)type II.

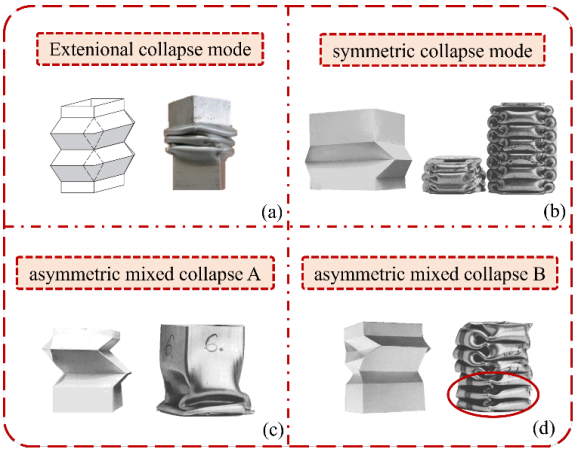

Fig. 3 Folding patterns of box-shaped tubes under axial crushing[13, 15]

Through the combination of two element types, the crushing mode of box-shaped tubes can be divided into three types: extended collapse mode, symmetrical collapse mode, and asymmetric mixed collapse mode[13]. The elements of the four tube corners in the extended collapse mode all present the folding type of Type I, while all four tube corners extend outward in the tube segment, as shown in Figure 3(a); The symmetrical collapse mode is manifested as a Type II folding element in all four angles of the tube segment, in which the folding flap of the box-shaped tube is stacked in an orderly manner, and the inner concave and outer convex lobes are symmetrical with the axis of the section, as can be seen in Figure 3(b). There are two folding types of folding elements in mixed folding mode, one is that the stacking position is unchanged and the same tube segment (the same tube body height) occurs to form different types of folding elements, defined as type A, which is shown in Figure 3(c); The other is that the stacking position is changed, and there are different types of folding elements in different segments, defined as type B, as presented in Figure 3(d).

Table 2 Parameter relationships in the super-folding element theoretical model[14]

Symbol of parameter	Meaning of parameters	Parameter relation
H	Element height	Geometric basic parameter
h	Tube wall thickness	Geometric basic parameter
b	Folding radius of the flap	Geometric basic parameter
c1、c2	Element width	Geometric basic parameter
ψ_0	Half-angle between tube walls	Geometric basic parameter
α	Vertical inclination Angle of element surfaces	Geometric basic parameter
b_1、b_2	Face width of tubes	$b_1 = 2c_1; b_2 = 2c_2$
S	Horizontal travel distance of cell-center line	$S = 2Hcos\alpha$
β	Angle between tube surfaces and the tube corner line	$\beta = \arctan(\frac{\tan\alpha}{\sin\psi_0})$
γ	Deflection Angle of the tube corner line	$\gamma = \arctan(\frac{\tan\psi_0}{\sin\alpha})$
v	Speed of the center line of the element	$v = H\cos\alpha\dot{\alpha}$
σ_y	Yield stress of material	Material basic parameter
σ_u	Ultimate strength of material	Material basic parameter
n	Hardening coefficient of strain	Material basic parameter
σ_0	Equivalent flow stress	$\sigma_0 = \sqrt{\frac{\sigma_u\sigma_y}{1+n}}$
M_0	Equivalent yield moment	$M_0 = \frac{N_0 h}{4} = \frac{\sigma_0 h^2}{4}$

2.2 Calculation of Energy Consumption and Average Force of Folding Element

2.2.1 Development of the Theory of Super-folding Element

Based on the super-folding element theoretical model, Abramowicz, Wierzbicki, Jones et al.[14, 16] divided the energy consumption of folding elements into energy consumption of horizontal fixed hinge, energy consumption of toroidal shell stretching and energy consumption of vertical travelling hinge. The horizontal fixing hinge is formed at the mid-line of the folding elements. Being relatively fixed in its position, it is combined with the tube angle to divide the folding elements into four trapezoidal surfaces, whose energy consumption mode is mainly manifested as out-of-plane bending energy consumption; The vertical travelling hinge takes into the change of the bending and folding position of the tube angle into account, and the migration distance of the hinge is related to the degree of folding elements; The energy consumption in the toroidal shell is mainly due to the plastic deformation of the material under the influence of stretching. In this way, the formation of the toroidal shell is simplified to the process of the tube surface passing through the toroidal surface, ignoring the influence of bending energy. These three energy consumption modes are combined to obtain the calculation formula for the energy of the super-folding element.

The average axial crushing force predicted by the super-folding element theory is relatively consistent with the experimental data, which also proves the correctness of the theory. However, the folding element theoretical model originally proposed by the researchers did not consider the variability of the plastic hinge of the box-shaped tubes, and ignored the lateral movement of the tube angle, so there is still plenty of room for

improvement in the element model and the average force calculation. On the basis of the original element model, Abramowicz et al.[17] took the moving characteristics of the tube angle line into consideration when deriving the energy consumption formula, defining the mobilization area of the tube angle as the cone unfolded surface and calculated it by using the travelling hinge method. The improved super-folding element theoretical model is shown in Figure 4(a). In order to prove the accuracy of the improved super-folding theory, Abramowicz [18], who carried out a large number of axial compression experiments on box-shaped tubes, have succeeded in applying the theory to the crashworthiness and energy consumption optimization design of thin-walled energy absorbers with the assistance of computers.

The super-folding element theoretical model and theory have provided a comprehensive and accurate solution to the problem of axial crush energy consumption of box-shaped tubes, and researchers have subsequently verified and expanded the model through experiments and numerical simulations. Considering the non-ideality of the folded flap of the cellular structure, Mahmoudabadi et al.[19] obtained the approximate solution of the folding angle by numerical method, and the authors of this paper applied the Lagrangian multiplier method to solve the folding energy consumption formula, so as to obtain the theoretical model of average crushing force and half-wavelength (Figure 4(b)). This solution method that combines numerical solution and analytical solution, provides a novel idea for the study of complex energy consumption folding theory. Based on the results of the actual crushing experiment and finite element simulation of the box-shaped tubes, Malekshahi[20] found that the bending radius of the convex folding flap in symmetrical mode is twice the radius of the concave folding flap. In view of this, the authors of this paper propose the average force calculation formula for the concave and convex fraction of the folded flap and verify the high consistency of the load-displacement curve by finite element analysis method. When it comes to super-folding element theoretical model, there is much room for improvement in terms of its spatial structure and theoretical calculation. However, the accuracy of folding theory is approaching the real situation of the experiment in the process of improvement, and the calculation formulas for the folding energy consumption mode in the literature are shown in Table 3.

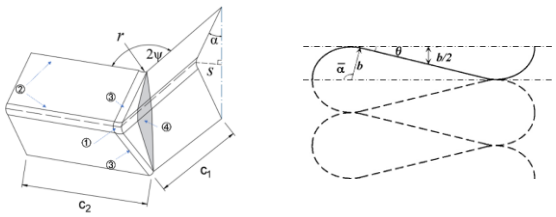

(a) (b)

Fig. 4 Improvements to the super-folding element theoretical model; (a) A super-folding model considering the unfolded surface of the cone; (b) Improvement in the bending angle of the folding flap[19]

Table 3 Calculation formulas for folding energy consumption of super-folding elements in literature

Literature	Types of energy consumption	Formulas	Features and improvements
Abramowicz et al.[14] (Fig. 1)	Toroidal shell	$E_{11}=4bHN_0I(\psi_0)=16HM_0I(\psi_0)b/h;$ $I_{11}(\psi_0)=\frac{\pi}{(\pi-2\psi_0)\tan\psi_0}\int_0^{\pi/2}\cos\alpha\{\sin\psi_0\sin(\frac{\pi-2\psi_0}{\pi})\beta+\cos\psi_0[1-\cos(\frac{\pi-2\psi_0}{\pi})\beta]\}d\alpha$	(a) first giving definition of the super-folding element theoretical model (b)assuming the non-coupling of the stretching and bending energy consumption of the film.
	Horizontal fixed hinge	$E_{12}=\pi M_0c_m$	
	Vertical travelling hinge	$E_{13}=\frac{4M_0H^2}{b\tan\psi_0}\int_0^{\pi/2}\frac{\cos\alpha}{\sin\gamma}d\alpha$	
Abramowicz et al.[17](Fig.3)	Toroidal shell①	E21=E11	Considering the contribution of energy consumption and average crushing force of the traverse hinge of the conical surface.
	Horizontal hinge ②	E22=E12	
	Toroidal shell③	E23=E13	
	Expanded cone surface④	$E_{24}=\frac{2M_0H^2\tan\psi_0}{h}\int_0^{\pi/2}\frac{\sin2\alpha}{1+\tan^2\psi_0\sin^2\alpha}d\alpha$	
Mahmoudabadi et al.[19]	Toroidal shell	$E_{31}=32M_0\frac{Hb}{h}I_1(\psi_0);$ $I_{31}(\psi_0)=\frac{\pi}{(\pi-2\psi_0)\tan\psi_0}\int_0^{\bar{\alpha}}\cos\alpha\{\sin\psi_0\sin(\frac{\pi-2\psi_0}{\pi})\beta+\cos\psi_0[1-\cos(\frac{\pi-2\psi_0}{\pi})\beta]\}d\alpha$	The formula for calculating the longitudinal folding angle is proposed as: $\bar{\alpha}=\frac{\pi}{2}+\frac{1}{2(H/b)-\pi}$

	Horizontal fixed hinge	$E_{32}=12M_0C\bar{\alpha}$	The value $\bar{\alpha}$ is obtained by the numerical method of being：1.7233.
	Vertical travelling hinge	$E_{33}=8M_0\frac{H^2}{b}I_3(\psi_0);$ $I_{33}(\psi_0)=\frac{1}{\tan\psi 0}\int_0^{\bar{\alpha}}\frac{\cos\alpha}{\sin\alpha}d\alpha$	
Malekshahi et al.[20]	Toroidal shell	$E_{41}(\alpha)=\frac{4Hb_1h}{\sqrt{3}\tan\psi_0}\{\sigma_yI_1+E_TI_2\};$ $I_{41}=\int_0^{\alpha}\beta(\alpha)\cos\alpha\cos\theta_1d\alpha;$ $A=\frac{3h\sin\psi_0}{b};\cos\theta_1=1-2\cos^2\alpha\cos^2\psi_0;$ $I_{42}=\int_0^{\alpha}\beta(\alpha)\cos\alpha\{\frac{1}{12}(2\cos\theta_1+A)\sqrt{\cos^2\theta_1+A^2+A\cos\theta_1}+\frac{1}{8}A^2\ln(\frac{A}{2}+\cos\theta_1+\sqrt{\cos^2\theta_1+A^2+A\cos\theta_1})-\frac{1}{12}A^2-\frac{1}{8}A^2\ln(3A)\}d\alpha$	(a) proposing that the outer folding radius is twice the inner folding radius; (b) providing definition of the modulus of linear plastic hardening by considering the plastic hardening effect of metallic materials: $E_T=\frac{\sigma_u-\sigma_y}{\varepsilon_u}$.
	Horizontal bending	$E_{42}(\alpha)=4\{\int_0^{\alpha}M^I(c_m+\frac{H\sin\alpha}{2\sin\psi_0})+M^O(c_m-\frac{H\sin\alpha}{2\tan\psi_0})\}d\alpha\}$ $M^I=\frac{2}{\sqrt{3}}(\frac{\sigma_yt^2}{4}+\frac{E_T\alpha t^3}{6\sqrt{3}b\alpha_f});M^O=\frac{2}{\sqrt{3}}(\frac{\sigma_yt^2}{4}+\frac{E_T\alpha t^3}{12\sqrt{3}b\alpha_f})$	
	Travelling hinge	$E_{43}(\alpha)=2\bar{M}_{rol}\frac{H^2}{b}\sin\psi_0\cot\gamma(\alpha)+\bar{M}_{rol}HI_3;$ $\bar{M}_{rol}=\frac{2}{\sqrt{3}}(\frac{\sigma_yt^2}{4}+\frac{E_T\sin\psi_0t^3}{12\sqrt{3}b});$ $I_{43}=2\int_0^{\alpha}(\frac{\pi-2\psi_0-2\theta_1}{\sin\gamma(\alpha)})d\alpha;$	

Note: where cm is the average width of the box-shaped tube cm = 1/2 (c1 + c2).

2.2.2 Expansion and Application of Superfolding Theory Calculations

Witnessing the development of automobile, aviation and other industries, great attention has been paid to the research of lightweight and efficient tubular energy consumption structures by researchers, for simple rectangular section metal tubes can no longer meet the requirements of design and application in reality[20, 21]. So far, the researchers have made progress in the theoretical development of the super-folding element and also provided key crashworthiness and energy consumption indicators for the optimal design of the tube body through exploring the optimal design of the axial crashworthiness and energy consumption capability of the tube body by increasing the lattice structure, changing the thickness of the tube wall, and using fillers in the box-shaped tubes. In the study of the spatial lattice form of box-shaped polytopic tubes, TrongGhan et al.[23] divided the angular elements in polytopic tubes into seven types: type of right angle, 3-type, T-type, crisscross type, 4-type, 5-type, and 6-type (as shown in Figure 5(a)), and calculated the energy consumption and average crushing force of each of the above types based on the super-folding element theoretical model. Subsequently, TrongGhan et al.[24] who optimized the type of polytopic box-shaped tube angle elements, reckoned that the stretching membrane energy of the tube surface when the angular element is deformed, is generated in the triangle intersecting along the 45 ° extension line of the tube angle (Figure 5(b)), and finally obtained a simplified calculation formula for the deformation energy consumption of the angular element. Yaozhong et al. [25] carried out research on the calculation of the crushing force of the variable intensity grid section with high angle element strength and low strength in the middle of the thin plate, in which the angle element of the segmented polytopic section is defined as corner element, T-shape element, and crisscross element (Figure 5(c)). These three types of angle element have different folded shapes. In this study, the authors have clarified the effective length of the angular element, calculated the value of the average crushing force, as well as verified the theoretical accuracy and obtained better base cell parameters through finite element simulation of axial compression of box tubes with different base cell numbers. According to the experimental results of polytopic tube structures in the literature, it can be concluded that the introduction of spatial lattice immensely improves the impact resistance and energy consumption efficiency of box-shaped tubes[26-28]. Besides, the spatial lattice can greatly enhance the stability of the box-shaped tubes and their torsional and flexural stability which are also the most concerned design indexes in engineering application.

The selection of box section filler needs to meet the requirements of suitable strength, good energy

consumption capability and excellent durability in terms of design. The common fillers used for buffering in the study tend to be materials with excellent energy consumption properties like ductile metals or polymers on the matrix, while in terms of structure, the spatial forms with good crushing response and cushioning capability are frequently used, such as the foam structure of polyurethane and aluminum foam [29-32] (Fig. 6(a)), the cellular structure of honeycomb aluminum [33-36] (Fig.6 (b)), as well as the spatial arrangement and lattice structure [37-39] (Fig. 6(c)), etc. As far as the crushing morphology and spatial variation are concerned, the crushing energy consumption and failure modes of each composite tube have different characteristics: for the randomness of the pore size of the filling material of the foam structures and the spatial distribution of its bubble particles, there is such a phenomenon that local bubble rupture failure generally occurs when subjected to axial load[29]. The antarafacial crushing mode of the cellular filling structure is similar to that of the box-shaped tube folding, that is, the energy is dissipated by folding through the plastic deformation of the cell wall. The spatial arrangement structure gives full play to the material properties by forming an angular and stretching space, which is divided into two stages during crushing, namely, spacial compression collapse and plastic deformation after dense. All in all, the application of filling buffer materials can improve the space utilization of the box-shaped tubes in an effective way, so it is an ideal method of combining the lattice form with the filling for box-shaped tube optimization.

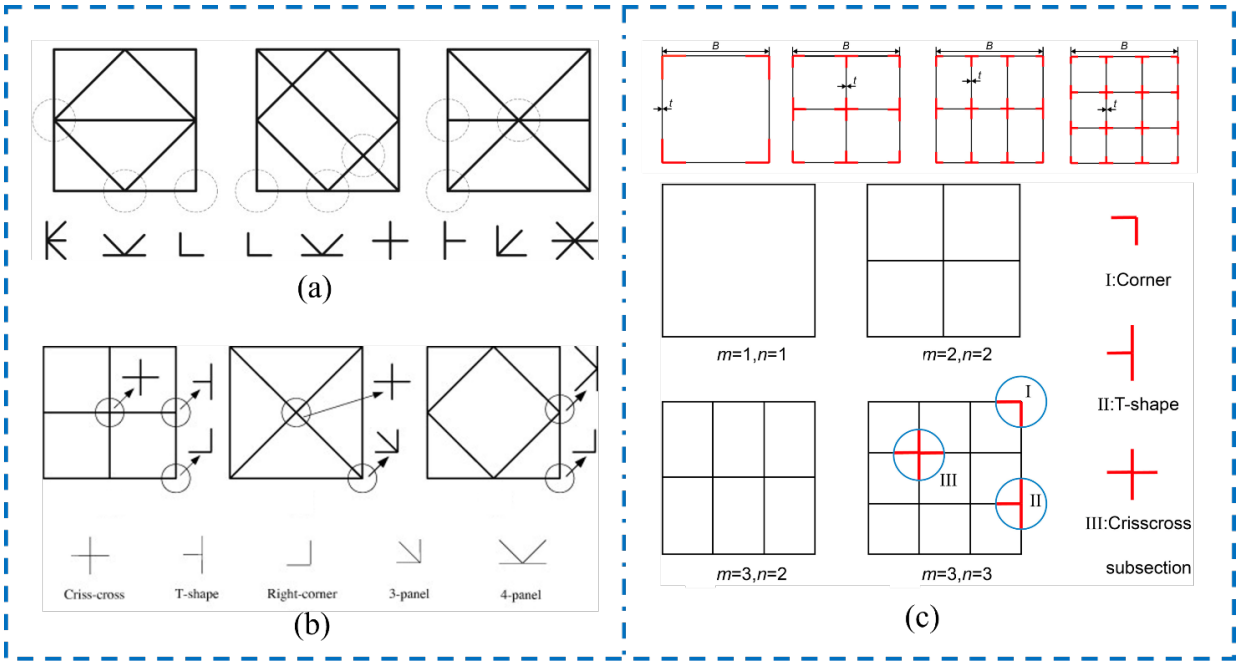

Fig. 5. Angular elements in different polytopic tubes; (a)Type of angular element[22]; (b)Type of simplified angular element[23]; (c)Angular element of variable cross-section of polytopic strength[24]

The selection of box section filler needs to meet the requirements of suitable strength, good energy consumption capability and excellent durability in terms of design. The common fillers used for buffering in the study tend to be materials with excellent energy consumption properties like ductile metals or polymers on the matrix, while in terms of structure, the spatial forms with good crushing response and cushioning capability are frequently used, such as the foam structure of polyurethane and aluminum foam [29-32] (Fig. 6(a)), the cellular structure of honeycomb aluminum [33-36] (Fig.6 (b)), as well as the spatial arrangement and lattice structure [37-39] (Fig. 6(c)), etc. As far as the crushing morphology and spatial variation are concerned, the crushing energy consumption and failure modes of each composite tube have different characteristics: for the randomness of the pore size of the filling material of the foam structures and the spatial distribution of its bubble particles, there is such a phenomenon that local bubble rupture failure generally occurs when subjected to axial load[29]. The antarafacial crushing mode of the cellular filling structure is similar to that of the box-shaped tube folding, that is, the energy is dissipated by folding through the plastic deformation of the cell wall. The spatial arrangement structure gives full play to the material properties by forming an angular and stretching space, which is divided into two stages during crushing, namely, spacial compression collapse and plastic deformation after dense. All in all, the application of filling buffer materials can improve the space utilization of the box-shaped tubes in an effective way, so it is an ideal method of combining the lattice form with the filling for box-shaped tube optimization.

The change of tube wall section thickness is also favored by researchers in optimization research, whether it is the study of thin-walled and box-shaped tubes with changing thickness [40-42] or the study of combined gradient [43], the basis for the change of tube wall thickness is derived from the uneven stress distribution characteristics of the tube section. According to the

effective cross-sectional method, when the aspect ratio is in a large degree, the stress level in the middle of the box-shaped tubes under the same axial force is significantly smaller than that of the angular element. It can be seen that the general optimization method is that the angular element will gradually make the thickness of the thin wall decreased as it approaches the middle position, which can be confirmed by the optimization results of the previous literature, as well. Compared with filling the buffer structure or increasing the spatial lattice, this method with limited effect of changing the cross-section of the tube wall is more of acting a role in optimization and improvement, so its overly complex thickness change makes the calculation workload increase.

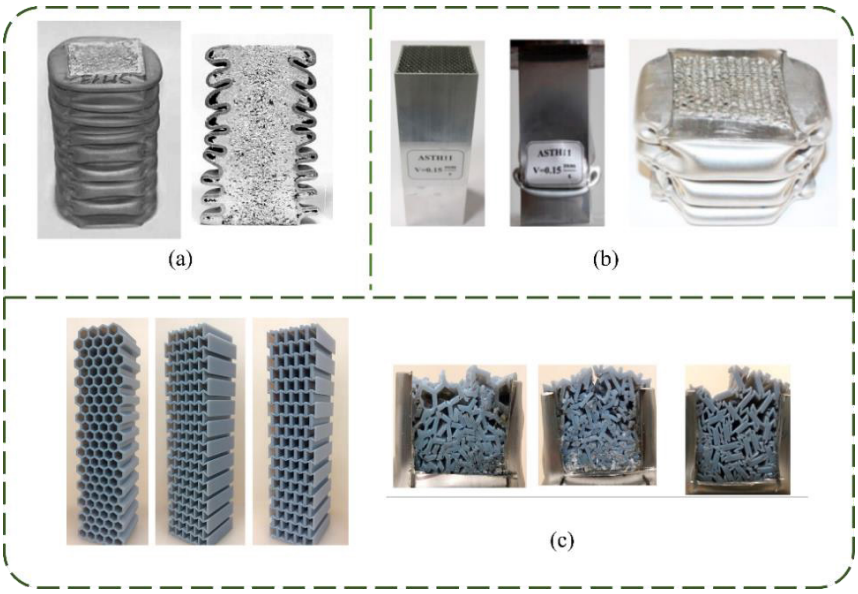

Fig. 6 Classification of box-shaped filled tubes
(a)Foam structure [32]; (b) Filling of cellular structure [33] ;(c) Spatial arrangement structure [39]

3. Critical Crushing Force of Box-shape Tube

When buffer structures such as box-shaped tubes exert their own energy consumption performance, the tube body gives full play to energy consumption in the plastic buckling stage. In contrast, it has a shorter duration in the elastic stage, and its crushing force response rises greatly, with the peak value formed often being greater than that in the plastic buckling stage. The initial peak force of the axial crush of the box-shaped tubes can reflect the ultimate bearing capacity of the tubes within the elastic range in the initial stage, which is an important research parameter for analyzing the crashworthiness of the tubes. On the one hand, the formation of the peak initial crushing force is related to the initial stiffness of the box-shaped tubes. The ratio of it to the average crushing force is called the crushing force efficiency (CEF), which is a reference index for studying the stability and energy consumption efficiency of the box-shaped tubes. On the other hand, when the peak force loading wave is transmitted to the protected components, its damage should be reduced as much as possible to the range that the protected components can withstand [44], so as to prevent premature partial destruction of the protected components. Therefore, the calculation theory of the peak crushing force plays an indispensable role in the overall design and analysis of box-shaped tubes.

3.1 Theory of Thin Plate Bending

The elastic plastic deformation of the box-shaped tubes in the initial folding stage belongs to the category of micro deformation. Due to the large initial stiffness of the metal material, micro deformation of the box-shaped tubes can lead to a rapid increase in cross-sectional stress. When the loaded energy reaches the elastic energy storage limit of the box-shaped tubes, it begins to appear a significant large deformation, which is manifested as tube surface buckling from a macroscopic perspective. At present, the calculation methods of critical buckling force of box-shaped tubes based on theory of plate bending mainly include: (1) Hencky-Nadai plastic deformation theory [45]; (2) Lévy–Mises theory of plastic flow[46], both of which assume the invariance of material volume in the discussion of plastic deformation [47]. Based on this assumption, both plastic flow theory and deformation theory are called J2 theory. Stowell et al. [48, 49] proposed a more comprehensive computational theory of plate plastic buckling, which took into account the influence of Poisson's ratio change, and preliminarily established the general differential equation for stability of thin plate. Vincenzo et al. [50], who adopted J2 theory and fully considered the plastic kinematic of Poisson's ratio of materials, proposed a critical buckling correlation equation for thin plates that conforms to the boundary conditions and characteristics of box-shaped tubes. Comparing the experimental results,

it is found that the buckling force obtained by considering the variability of the Poisson's ratio is closer to the experimental value (Table 5). The application of theory of thin plate bending can accurately solve the critical stress and external micro-deformation of the box-shaped tube, and meet the solution requirements under any boundary conditions and constraints. However, the fact is that the use of elastic plastic mechanics methods often requires a more complex partial differential equation derivation and complex calculation, and it is not an easy job to know the box tube boundary constraints, so this method cannot be effectively popularized and applied in engineering.

3.2 Effective Cross-sectional Method

In the design of large-scale projects in the construction industry, such components as box-shaped beams and box-shaped columns, with huge computational effort, the calculation process of theory of thin plate bending is too complex. Therefore, an alternative method for calculating the ultimate bearing capacity which is simple, efficient and accurate are being needed. After repeated experiments and calculations, VonKarman et al. proposed an effective cross-sectional method based on the ideal thin plate bending equation. When the box-shaped component is compressed in its axial direction, the stress distribution on its cross-section is not uniform, which is manifested in the fact that the stress at its corner is greater than that in the middle part of the plate wall of the component (Fig. 7(a)). The effective cross-sectional method is used to make the stress distribution of the original box section equivalent to a uniform distribution of the maximum stress by the edge, as shown in Fig.7 (b). Because the effective cross-sectional method is not only simple to calculate, but also convenient to obtain its parameters, the specifications of the construction industry and machinery industry in various countries gradually adopt this method in the calculation of the ultimate bearing capacity of section steel structures and metal components of box sections. The size of the effective area enclosed by the equivalent width be whose value is related to the material strength and critical buckling stress, can reflect the force uniformity of the cross-section to some degree. In the elastic plastic theory, the local critical buckling stress σ_{cr} of the independent thin plate is affected by the height of its cross-section and the width of the plate, whose expression is shown as follows:

$$\sigma_{cr} = \frac{k\pi^2 E}{12(1-\nu^2)(B/h)^2} \tag{1}$$

where k refers to the stability factor of the plate, E is the Young's modulus of the material, B is the width of the square sheet, and ν is the Poisson's ratio of the material. In the American AISI design code, it specifies the critical buckling force of the axial stress components of the box section calculated by the effective cross-sectional method, and the critical buckling force of the set section is calculated by the formula after defining the effective width of the parameter λ:

$$\rho = \begin{cases} 1 & \lambda \le 0.673 \\ (1-\dfrac{0.22}{\lambda})/\lambda & \lambda > 0.673 \end{cases} \tag{2}$$

$$b_e = \rho B \tag{3}$$

$$P_{cr} = N\sigma_y h b_e \tag{4}$$

The critical stress σcr discussed above for effective width calculation is based on the ideal critical stress under the unconstrained independent thin plate, but the components of the box section must be constrained by adjacent plates under the action of axial force, and there may occur coupling phenomena of two or more buckling modes between adjacent plates, which will lead to inaccurate critical stress calculation, thereby affecting the predicted value of subsequent critical forces.

In the European standard EN1999-1-1[51], it considers the stress flow of material, the interaction between plates of box section, as well as the nonlinear behavior of materials in the calculation method of critical strength, and introduces multiple coefficients to modify the critical stress. In Table 4, the values of the corrected parameters suitable for box section tubes are extracted, and the corrected plastic critical stress calculation formula is presented as follows:

$$\sigma_{cr}' = \frac{\xi\zeta\alpha_{LS} k\pi^2 E}{12(1-\nu^2)(B/h)^2} \tag{5}$$

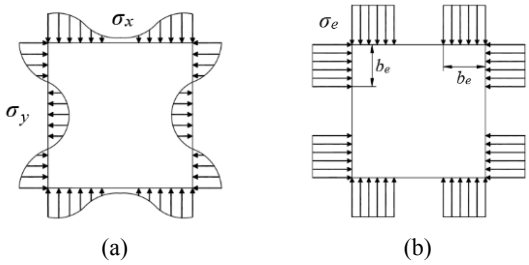

Fig. 7 Axial compressive stress distribution of box section (a) Stress distribution in the limit state; (b) Distribution of equivalent stress

Table 4 Corrected parameters for critical stress in the Eurocode (EN1999-1-1)

Correction Factor	Value and Calculation Method	Notes
ζ	For box sections: $\zeta = 1.75 - \dfrac{0.45 b_2/b_1}{0.15 + b_2/b_1} - 0.02275(b_2/b_1)^3 \ge 1$	Considering the modification of mutual restraint between adjacent surfaces on the box section; b1 and b2 are the width of the tube surface.

ξ	$\xi = \frac{E_S}{E}(\frac{n-8}{n} + \frac{8}{n}\sqrt{\frac{E_t}{E_S}})$	n refers to the hardening index of the Ramberg-Osgood stress-strain curve formula; E_t and E_S are the tangential modulus and secant modulus of the material, respectively.
α_{LS}	For pressure-receiving surface of inward concave: $\alpha_{Ls} = 1 + \frac{0.425}{(Ls/B)^{0.75} - 0.2}$; For pressure-receiving surface of outward concave: $\alpha_{Ls} = 1 + \frac{4}{(Ls/B)^{0.95} - 0.6}$	Considering the degree of influence of longitudinal stress gradient; Ls is the shear length, which is the distance from the zero bending moment point to the maximal bending moment point on the cross-section; b is the width of the sheet compression; If the cross-section belongs to uniform compression, taking it as $\alpha_{Ls} = 1.0$.
k	For the box section, the researchers obtained it after summarizing a large number of experimental data: k=4.0[50]	Considering the modification of boundary constraint effects
v	$v = v_p - \frac{E_t}{E_S}(v_p - v_e)$	Poisson's ratio variability of plastic materials[50]

The corrected critical stress is more accurate and closer to the actual engineering situation. Vincenzo et al.[50] conducted a large number of axial compression experiments on box section aluminum tubes of 6060 T6 material. By comparing the calculation formula of thin plate bending theory and EN1999-1-1 critical stress theory, they found that the error between the theoretical and experimental values in the two theoretical calculation methods is small (in Figure 8(a)(b)), and the deviation degree of the two theories is similar (in Table 5). It also can be concluded that the effective cross-sectional method, with high accuracy in calculating the critical force of box section tubes, is feasible and effective in practical application.

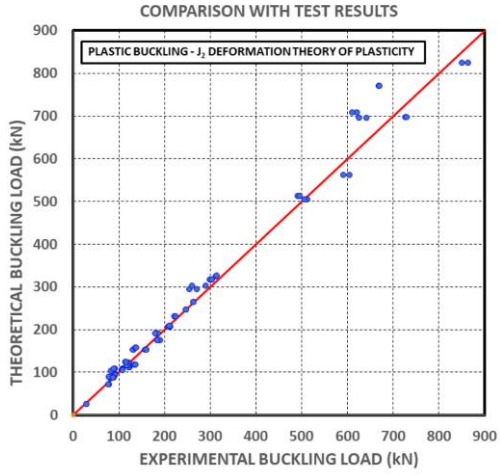

(a)

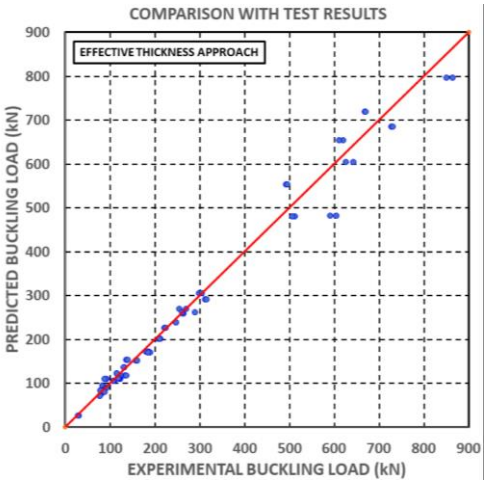

(b)

Fig. 8 Comparison of experiment and theory[50]; (a) Critical forces derived from experiment and thin plate buckling theory; (b) Critical forces obtained by experiment and effective cross-sectional methods

Table 5 Comparison of theoretical and experimental values[50]

	Plate buckling theory—EXP		**Effective Cross-sectional Method—EXP**
Poisson's ratio variability	×	√	×
$N_{u,th} / N_{u,\exp}$	1.051	1.01	0.97
Standard deviation	0.121	0.089	0.081

Although the effective cross-sectional method for critical stresses is easy to calculate, there are still inaccurate calculations when it comes to more complex cross-sectional forms. In order to compensate for the limitations of the effective cross-sectional method, the researchers propose a direct strength method suitable for calculation in more complex situations, in which it unifies the effective width method, replacing the

effective width with effective bending strength and effective buckling force, so that complex force conditions such as bending, shearing and torsion of components can be considered more comprehensively. However, being a semi-theoretical and semi-empirical computational model, it is highly targeted. As a consequence, a lot of experimental and theoretical research is needed when the key parameters in the complex cross-section and buckling modes are concerned[52, 53].

Since the axial compression state of the box section tube is relatively simple and its cross-section is straight and regular, it is feasible and effective to use the effective cross-sectional method to calculate the critical crushing force of the tube body. Therefore, combined with the comprehensive analysis of the computation and accuracy of thin plate bending theory, effective cross-sectional method, as well as direct strength method, it can be seen that the effective cross-sectional method is the best one for the analysis of critical buckling force of box section tubes.

4 Application Prospect of Thin-walled Box-shaped Tube in Civil Engineering

In practical engineering, engineers and researchers are more likely to apply thin-walled box-shaped tubes to the anti-collision cushioning of automobiles, ships, aircraft and other vehicles. Currently, the application of thin-walled box section tubes is more common in the field of automotive engineering. Regarding the frame design of the automobile, it pursues light weight, high strength and high protection[54], while the thin-walled tube and its various spatial changes make it flexible to adapt to the requirements of the shape design of the car. In addition, the lightweight metal box tube can not only provide sufficient overall rigidity for the car, but also dissipate a large amount of impact energy in time in the event of an impact accident, which is quite suitable for being made into a protective beam and frame support column of the car, as shown in Figure 9 of the application of the box-shaped tubes in the vehicles [55].

With the rapid development of the transportation industry, it has witnessed the gradual increase in transportation volume, and the risk of important load-bearing structural components such as bridge structures, especially bridge piers, being hit by vehicles and ships, is also on the increase. Therefore, it is an important means to protect or mitigate the damage of the bridge in traffic accidents by attaching external buffer protection devices to the surface of the bridge pier components. Impact protectors in bridge engineering need to have higher energy consumption capability and impact resistance than those of automobile energy absorbers. As far as thin-walled box-shaped tube is concerned, it can obtain a composite tube with excellent buffer energy consumption ability by filling buffer materials, increasing lattice structures or forming spatial arrangements. Compared with the traditional concrete protective components, its mass is significantly smaller under the same protective strength of the thin-walled box-shaped tubes, which can effectively reduce the load of the bridge piers and is also easy to replace and inspect. In comparison to the anti-collision devices formed by high polymer represented by polyurethane alone, the box-shaped tube wall can effectively protect the internal buffer, thereby preventing the buffer from aging and invalidating. In addition, under the enclosure of the tube wall, the collision resistance of the whole tube can be enhanced by coupling between the buffer filling and the thin wall, and the buffer under confining pressure can maximize its buffering efficiency, so that the combined structure of the box tube can show a more efficient buffer process when impacted.

In the protection engineering of bridges and other buildings, box section tubes are usually combined to form a collision avoidance box system to cope with anti-collision conditions. Being different from the anti-collision devices of automobiles, the protected objects of civil engineering protective devices are generally components with high stiffness such as piers, beams and columns, which attach great importance to the efficiency and performance of the collision avoidance system, and the specific differences between them and the anti-collision requirements of automobiles are shown in Table 6. On the whole, automobile collision avoidance materials or their combined structural forms can be used for bridge impact protection, but they differ in emphasis on use requirements.

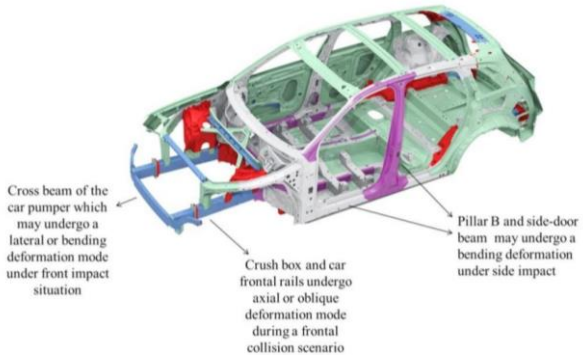

Fig. 9 Application of box-shaped tubes in automobile protection[55]

Table 6 Differences between engineering protection and automobile protection

Item	Automobile Protection	Civil Engineering Protection
Protected Objects	human and engine	bridge piers, beams, columns and other components
Protection Requirements	Minimizing or eliminating impact energy transfer to protect the human body or engine from injury[40];	The component should be guaranteed to respond within the elastic range as much as possible[56,57].

Protective Position	In the event of an accident, the engine and crew compartment should be surrounded by a crease area as much as possible to achieve the goal of effective protection[21].	Protection should be carried out in vulnerable parts, the characteristics of which are related to changes in water level (ship-bridge) and the height range of vehicle impact point (vehicle-axle)[57-59].
The strength and stiffness of the protection device	The design benchmark is based on the anti-collision energy required under the specified stroke[60].	It needs to consider the degree of damage to the pier under the specified impact energy in the process of design; Considering the adaptability of the collision avoidance device to the stiffness of the piers[58]
Energy Transfer	Weakening it as much as possible and dissipating in other forms[60,61]	Transferring it appropriately and allowing the piers to receive and dissipate energy within the elastic range;
Stress Transfer	By setting bending zones to make stress transfer away from the human body[61]	The stress is transferred through the contact areas between the anti-collision boxes and the piers[58].

When it comes to application of the excellent energy consumption properties of box section tubes in civil engineering, there are still some challenges. (1) In civil engineering protection, the buffer is required to have greater strength and better collision resistance, and the structural optimization also needs to be based on the stiffness of the components and the allowable energy transfer, which makes the box section tubes need to be adjusted to a better space structure to meet the protection requirements. (2) The buffer used for civil engineering protection has a large installation space, and it does not require the buffer to make a specific special-shaped device, which can ensure the uniformity of the tube body. However, the volume of protected objects such as bridge piers, beams and columns is relatively large, and the box section tube is combined to form an collision avoidance system, so its arrangement and overall stability still need to be studied in depth. (3) The box tubes used for sea bridge protection needs to ensure its tightness and corrosion resistance, and materials like stainless steel metal with high strength and great corrosion resistance and CFRP can be used for the study of anti-collision performance in this regard.

5 Conclusion

In this paper, the theory and its expansion and application of box section tubes under axial loading are reviewed as a whole. First and foremost, it summarizes of the formation and improvement of the calculation theory of energy consumption and average force under axial crushing of box section tubes, expands the internal spatial form and buffer filling method of box section tubes, and expounds the spatial diversity and application flexibility of box section tubes in this paper. Moreover, as to the calculation of critical buckling force, it gives an introduction to the three methods the elastic plastic thin plate bending theory, effective cross-sectional method as well as direct strength method. In combination with relevant literature, it makes a comparison of these three methods by referring to the cross-sectional method calculation formula proposed in the European standard EN1999-1-1 and the American standard AISI in this paper. Ultimately, it compares the differences between automobile protection and bridge protection, and analyzes the use of box-shaped tubes in automobiles and its application prospect in the field of impact protection in civil engineering in this paper. The conclusions are as follows:

1. The research and development of super-folding theory is already in a relatively mature stage. However, due to the complexity of the spatial structure, the researchers have simplified the division and calculation of the energy-consuming area of the unit space, so a more detailed division and calculation is being needed.
2. There is a greater enhance in the overall stability and crashworthiness of the box section tubes after increasing the lattice structure, while the fillers are capable of enhancing the compactness and cushioning capability of the tube body, so the box-shaped tubes can have better performance by increasing the lattice structure, filling the buffers and other optimization methods;
3. Compared with the thin plate bending theory and direct strength method, the parameter values of the effective cross-sectional method are not only clear and easy to obtain, but also its calculation process is simple, and the critical force calculation results for the box section are accurate, which can be regarded as the optimal critical force calculation method among these three methods;
4. The application of box-shaped tubes in bridge structural protection is feasible, and there is great room for development and improvement, and it is necessary to solve key technical and design problems such as strength adaptation, pipe fitting assembling and installation.

Declaration of conflicting interests

The authors declared no potential conflicts of interest with respect to the research, authorship, and/or publication of this article.

Acknowledgment

Funding: This work was supported by the Characteristic Innovation Project of Guangdong Universities (Project Number: 2020KTSCX128) and Foshan University Student Academic Fund (Grant xsjj202211kjb04).

References

1. Sofuoglu H, cam S. (2021) Coupled effect of thickness optimization and plastic forming history on crashworthiness performance of thin-walled square tube. NT J ADV MANUF TECH. 117(9-10): 2935-2948.

2. Tran T. (2020) Study on the crashworthiness of windowed multi-cell square tubes under axial and oblique impact. THIN WALL STRUCT. 155.
3. Mohsenizadeh S, Ahmad Z, Alias A. (2020) Numerical Prediction on the Crashworthiness of Circular and Square Thin-Walled Tubes with Polymeric Auxetic Foam Core. JOURNAL OF J MATER ENG PERFORM. 29(5): 3092-3106.
4. Han J, Yamazaki K. (2003) Crashworthiness optimization of S-shape square tubes. INT J VEHICLE DES. 31(1): 72-85.
5. Guillow S, Lu G, Grzebieta R. (2001) Quasi-static axial compression of thin-walled circular aluminium tubes. INT J APPL MECH. 43(9): 2103-2123.
6. Xiang Y, Wang M, Yu T. et al. (2015) Key performance indicators of tubes and foam-filled tubes used as energy absorbers. INT J APPL MECH. 7(04): 1550060.
7. Song Z, Ming S, Li T. et al. (2021)Improving the energy absorption capacity of square CFRP tubes with cutout by introducing chamfer. INT J MECH SCI.1, 189.
8. Bodlani S, Yuen S C K, Nurick G. (2009) The energy absorption characteristics of square mild steel tubes with multiple induced circular hole discontinuities—part I: experiments.
9. Pratama A A, Prabowo A R, Muttaqie T. et al. (2023) Hollow tube structures subjected to compressive loading: implementation of the pitting corrosion effect in nonlinear FE analysis. J BRAZ SOC MECH SCI. 45(3).
10. Xu P, Wang D, Yao S. et al. (2021) Multi-objective uncertain optimization with an ellipsoid-based model of a centrally symmetrical square tube with diaphragms for subways. STRUCT MULTIDISCIP O. 64(4): 2789-2804.
11. Abdullahi H S, Gao S. (2021) A two-stage approach to the optimization design of multi-cell square tubal structures. STRUCT MULTIDISCIP O. 63(2): 897-913.
12. Li Z, Rakheja S, Shangguan W-B. (2020) Crushing behavior and crashworthiness optimization of multi-cell square tubes under multiple loading angles. P I MECH ENG D-J AUT. 234(5): 1497-1511.
13. Abramowicz W, Jones N. (1984) Dynamic axial crushing of square tubes. INT J IMPACT ENG. 2(2): 179-208.
14. Wierzbicki T, Abramowicz W. (1983) On the crushing mechanics of thin-walled structures.
15. Menouer A, Baleh R, Djebbar A. et al. (2014) New generation of energy dissipating systems based on biaxial buckling. THIN WALL STRUCT. 85: 456-465.
16. Abramowicz W. (1983) The effective crushing distance in axially compressed thin-walled metal columns. INT J IMPACT ENG. 1(3): 309-317.
17. Abramowicz W. (1997) The macro element approach in crash calculations. Crashworthiness of transportation systems: structural impact and occupant protection. 332: 291-320.
18. Abramowicz W. (2003) Thin-walled structures as impact energy absorbers. THIN WALL STRUCT. 41(2-3): 91-107.
19. Mahmoudabadi M Z, Sadighi M. (2011) A theoretical and experimental study on metal hexagonal honeycomb crushing under quasi-static and low velocity impact loading. MET SCI ENG A. 528(15): 4958-4966.
20. Malekshahi A, Shirazi K, Shishehsaz M. (2019) Axial crushing of prismatic multi-corner metal columns considering plastic hardening and curvature. J MECH. 35(3): 315-326.
21. Bhutada S, Goel M D. (2021) Crashworthiness parameters and their improvement using tubes as an energy absorbing structure: an overview. INT J CRASHWORTHINES
22. Patel V, Tiwari G, Dumpala R. (2020) Review of the crushing response of collapsible tubular structures. FRONTIERS OF MECH ENG. 15(3): 438-474.
23. TrongNhan T, Hou S, Han X. et al. (2014) Theoretical prediction and crashworthiness optimization of multi-cell square tubes under oblique impact loading. INT J MECH SCI. 89: 177-193.
24. TrongNhan T, Hou S, Han X. et al. (2015) Crushing analysis and numerical optimization of angle element structures under axial impact loading. COMPOS STRUCT, 2015, 119: 422-435.
25. Wu Y, Fang J, Cheng Z. et al. (2020) Crashworthiness of tailored-property multi-cell tubular structures under axial crushing and lateral bending. THIN WALL STRUCT. 149: 106640.
26. Li Z, Ma W, Xu P. et al. (2019) Crushing behavior of circumferentially corrugated square tube with different cross inner ribs. THIN WALL STRUCT. 144.
27. Ferdynus M, Kotełko M, Urbaniak M. (2019) Crashworthiness performance of thin-walled prismatic tubes with corner dents under axial impact-Numerical and experimental study. THIN WALL STRUCT. 144: 106239.
28. Nia A A, Attar A A. (2017) The effect of different layouts in internal and external stiffeners on the energy absorption of thin-walled structures with square sections. ARCH CIV MECH ENG 17(4): 997-1010.
29. Wang G, Zhang Y, Zheng Z. et al. (2022) Crashworthiness design and impact tests of aluminum foam-filled crash boxes. THIN WALL STRUCT. 180.

30. Rogala M, Ferdynus M, Gawdzinska K. et al. (2021) The Influence of Different Length Aluminum Foam Filling on Mechanical Behavior of a Square Thin-Walled Column. MATERIALS. 14(13).
31. Yang X, An T, Wu Z. et al. (2020) The effect of outer tube on quasi -static compression behavior of aluminum foam -filled tubes. COMPOS STRUCT. 245.
32. Seitzberger M, Rammerstorfer F G, Gradinger R. et al. (2000) Experimental studies on the quasi-static axial crushing of steel columns filled with aluminium foam. INT J SOLIDS STRUCT. 37(30): 4125-4147.
33. Hussein R D, Ruan D, Lu G. et al. (2017) Crushing response of square aluminium tubes filled with polyurethane foam and aluminium honeycomb. THIN WALL STRUCT. 110: 140-154.
34. Wang Z, Yao S, Lu Z. et al. (2016) Matching effect of honeycomb-filled thin-walled square tube-Experiment and simulation. COMPOS STRUCT. 157: 494-505.
35. Hussein R D, Ruan D, Lu G. et al. (2016) Axial crushing behaviour of honeycomb-filled square carbon fibre reinforced plastic (CFRP) tubes. COMPOS STRUCT. 140: 166-179.
36. Yin H, Wen G, Hou S. et al. (2011) Crushing analysis and multiobjective crashworthiness optimization of honeycomb-filled single and bitubular polygonal tubes. MATER DESIGN. 32(8-9): 4449-4460.
37. Ma F, Liang H, Pu Y. et al. (2022) Crashworthiness analysis and multi-objective optimization for honeycomb structures under oblique impact loading. INT J CRASHWORTHINES. 27(4): 1128-1139.
38. Zhang Z, Liu S, Tang Z. (2011) Comparisons of honeycomb sandwich and foam-filled cylindrical columns under axial crushing loads. THIN WALL STRUCT. 49(9): 1071-1079.
39. impson J, Kazanc Z. (2020) Crushing investigation of crash boxes filled with honeycomb and re-entrant (auxetic) lattices. THIN WALL STRUCT. 150.
40. Sun G, Pang T, Xu C. et al. (2021) Energy absorption mechanics for variable thickness thin-walled structures. THIN WALL STRUCT. 118: 214-228.
41. Zhou J, Qin R, Chen B. (2019) Energy absorption properties of multi-cell thin-walled tubes with a double surface gradient. THIN WALL STRUCT. 145.
42. Zhou J, Qin R, Chen B. (2019) On the Folding Mechanics of Square Columns with Double-Surfaced Gradients. MATH PROBL ENG.
43. Zhou J, Dong C, Wang Z. et al. (2022) Approaching ideal energy absorption through the multicellular structure with gradient material distribution. INT J MECH SCI. 225.
44. Langseth M, Hopperstad O. (1997) Local buckling of square thin-walled aluminium extrusions. THIN WALL STRUCT. 27(1): 117-126.
45. Molotnikov V, Molotnikova A, Molotnikov V. et al. (2021) Plasticity Theory of Henky–Nadai–Ilyushin. Theory of Elasticity and Plasticity: A Textbook of Solid Body Mechanics. 195-217.
46. Firat M. (2008) An analysis of sheet drawing characteristics with drawbead elements. COMP MATER SCI 41(3): 266-274.
47. Gotoh M. (1998) A numerical study of various plastically unstable behaviors in tension and compression. MATER MET. 4: 628-639.
48. Stowell E Z. (1984) A unified theory of plastic buckling of columns and plates.
49. Stowell E Z. (1950) Compressive strength of flanges. National Advisory Committee for Aeronautics.
50. Piluso V, Pisapia A. (2021) Interactive plastic local buckling of box-shaped aluminium members under uniform compression. THIN WALL STRUCT. 164: 107828.
51. Draft BS EN1999-1-1. (2021) Eurocode 9: Design of aluminium structures - Part 1-1: General structural rules. European Committee for Standardization.
52. Chen S, Fang H, Liu J-z. et al. (2022) Design for local buckling behaviour of welded high strength steel I-sections under bending. THIN WALL STRUCT. 172: 108792.
53. Liu J-z, Fang H, Chan T-M. (2023) Numerical investigation on local buckling behaviour of cold-formed high strength steel irregular hexagonal hollow section stub columns. THIN WALL STRUCT. 185: 110571.
54. Garai F, Beres G, Weltsch Z. (2020) Development of tubes filled with aluminium foams for lightweight vehicle manufacturing. MAT SCI ENG A-STRUCT790.
55. Baroutaji A, Sajjia M, Olabi A-G. (2017) On the crashworthiness performance of thin-walled energy absorbers: Recent advances and future developments. THIN WALL STRUCT. 118: 137-163.
56. Chen G, Huang H, Xiang Z. (2022) Study on the Anticollision Performance of a New Corrugated Steel Protection System for Bridge Pier. SHOCK VIB..
57. Fan W, Shen D, Zhang Z. et al. (2020) A novel UHPFRC-based protective structure for bridge columns against vehicle collisions: Experiment, simulation, and optimization. ENG STRUCT.
58. Jiang H, Chorzepa M G. (2016) Case Study: Evaluation of a Floating Steel Fender System for Bridge Pier Protection against Vessel Collision. J BRIDGE ENG. 21(11).

59. Chen G, Huang H, Xiang Z. (2022) Experiment and Simulation on the Anticollision Performance of a New Corrugated Steel Protection System for Bridge Piers. SHOCK VIB.
60. Li Q Q, Li E, Chen T. et al. (2021) Improve the frontal crashworthiness of vehicle through the design of front rail. THIN WALL STRUCT. 162.
61. Pyrz M, Krzywoblocki M, (2022) Wolska N. Optimal crashworthiness design of vehicle S-frame using macro-element method and evolutionary algorithm. STRUCT MULTIDISCIP O. 65(3).